CrossMark

TECHNICAL ARTICLE—PEER-REVIEWED

A Case Study on Fatigue Failure of a Transmission Gearbox Input Shaft

M. Haghshenas · W. Savich

Abstract In this paper, a root cause analysis of premature failure of a gearbox input shaft, manufactured of AISI 1045-H, was performed through standard procedures for failure analysis. Shaft failed on cross oil hole through a helical fracture and therefore did not meet bogie 100,000 cycles during the verification with 10 Hz frequency cyclic testing. The fracture in the oil hole implied evidence of fatigue (i.e., beach marks on the fracture surface were clearly visible). Prior to improving the fatigue life and suggesting required remedial actions, mechanism of failure has to be understood, especially the initiating point of cracking. To this end, chemical analysis, microstructural characterization, fractography, hardness measurements, and finite element simulation were used to assess the nature of fracture in detail. The fractography analysis showed that fatigue beach marks originate from transition zone of the case on the cross oil hole. This is possibly due to the fact that torsional strength in this area is lower than torsional fatigue strength which leads to fatigue crack initiation, crack growth, and final fracture. At the end of this paper, proper remedial actions have been proposed.

Keywords Fatigue · Failure · Gearbox input shaft · Torsional strength · Tempered martensite

M. Haghshenas (✉)
Department of Mechanical Engineering, University of North Dakota, Grand Forks, ND, USA
e-mail: meysam.haghshenas@engr.und.edu

W. Savich
Frank Hasenfratz Centre of Excellence in Manufacturing, Linamar Corporation, Guelph, Canada

Introduction

It is estimated that one-quarter of all automotive failures belongs to the failure of vehicle's drivetrain [3]. Among different engine components, gearbox shafts that transmit motion from the differential to the wheels are normally subjected to large torsional and bending moments as well as cyclic stresses during actual service [1, 2]. These factors can effectively contribute to premature fatigue failure and fracture of the input shaft which results in replacement cost and engine downtime. The main reasons of these failures are flawed manufacturing, defective design, incorrect materials selection (or poor-quality raw material) as well as improper heat treatment (i.e., case hardening) [3, 4]. For instance, in a failure analysis of the end of a shaft of an engine by Atxaga and Irisarri [5], failure of the shaft was attributed to the combination of various factors including lack of strength, incorrect design and execution of the repair. Godec et al. [3] studied the fracture of a car's drive shaft machined from a case-hardened steel (25CrMo4). They attributed the premature failure to an incorrect selection of heat treatment parameters (i.e., austenitization temperature and tempering time). Xu et al. [1] investigated failure of a diesel engine gear shaft and reported multiple origin fatigue as the dominant failure mechanism of the gear shaft. Han [6] assessed fatigue failure on the keyway of the reduction gear input shaft connecting a diesel engine and inferred poor design of the shaft's keyway as the main reason for premature failure. Bhaumik et al. [7] studied fatigue failure of a hollow power transmission shaft; they attributed the fatigue crack to the stress concentrations resulting from the combined effect of improper machining and inadequate radius at the keyway end edges. In a recent study, Li et al. [8] assessed premature fracture of a military tank axle under torsional load. They

🍎 Springer

reported primary and secondary cracks on the axle and attributed the occurrence of final rupture to propagation of the primary and the secondary cracks to a certain level of the torsion axle that could not sustain the external load.

Normally, machined input shafts are case hardened to reduce the wear and improve fatigue life. Via induction hardening, the hardness (strength) near the surface improves which results in better fatigue life during torsional loading in which shear stress is maximum at the surface but negligible at the center of the shaft. Upon surface hardening, due to volume expansion of martensitic transformation, stress state at the surface will be in compressive mode, which further improves the fatigue life. For this application, the shaft does not need to be through hardened since the shear stress is negligible at the center, while hardening at the surface is required to exceed the applied stresses.

In the present study, failure of a transmission gearbox input shaft in the fatigue (cyclic) test is studied through experimental and simulation approaches. Quantitative methods, i.e., chemical analysis, microstructural characterization, fractography, hardness measurements, as well as finite element simulation, are employed to reveal the root of fracture in detail.

Experimental Procedure

To discover the root causes of the failure in the tested input shafts, the different steps were carried out in chronological sequence; first, the characteristics of the damage were documented through recorded digital images followed by visual inspection of damage using a stereomicroscope. Using standard metallography procedures, the specimens were polished for microhardness testing and etching. Case-depth hardness measurement was, then, taken through Vickers microhardness profiles using 1000 gf. The fractured specimen was then etched using 2% Nital solution for 5 s to assess the microstructure in the vicinity of substantial mechanical damage in the shaft. Using an advanced metallurgical microscope (MTI Corporation), the microstructure of the case and core was recorded. Using scanning electron microscopy (SEM) model Hitachi 3400N in backscattered electron mode, along with energy-dispersive X-ray (EDS) analysis, the fracture surface was studied at high magnifications. Finally, finite element simulation was performed to assess regions with stress concentration during actual service.

Results and Discussion

Fatigue Test

Using a MTS 215.51 heavy duty rotary system (Fig. 1), torsional fatigue test was performed on the shafts with the frequency of 10 Hz and angular displacement dynamic of 90° (+/−45°). Table 1 provides the fatigue tests that were performed on five input shafts. As shown in the table, one of the shafts passed slightly beyond 100,000 cycles and the rest failed in less number of cycles. The failure mode on all tested shafts was recorded as helical fracture through oil hole (Fig. 2). The fracture of the shaft shows that the crack originated at the position of key slot and evolved gradually, and finally, it led to a fracture and an edge-form 45° helical manners crack in the shaft. It also can be seen that the crack near the key slot is in a typical tooth form which is the typical characteristic of a torsional fatigue fracture. This shows that the fracture may be caused by the cyclic torsion moment in which the shaft is subjected to. Therefore, to measure the moment loaded on the shaft is necessary to verify the existence of cyclic load. Based on the test and measurement, the stress and strength then can be analyzed to assess the causes of the shaft fracture.

Microstructure and Fracture Surface

Figure 3 shows the microstructure of the alloy in the core region and in the case. The structure of the case, which has been hardened, consists of bainite/tempered martensitic which is quite typical and desirable for the case. The microstructure in the core, however, consists of pearlite/ferrite and some retained austenite. The white regions represent ferrite which are surrounded by pearlite (a layered phase). This microstructure agrees with the carbon content of the AISI 1045 steel.

Unlike bending fatigue, torsional fatigue causes excessive twisting that fails the part. Beach (ratchet) marks at the fracture initiation point can be observed in the fractured surface. Figure 4 shows the stereomicroscope image of fracture surface of the shaft damaged by torsional fatigue (both sides of the oil hole have been presented here which shows similar crack initiations). As seen, fatigue fracture starts from the cross oil hole and propagate perpendicular to the hole. The image shows that the river marks (shown
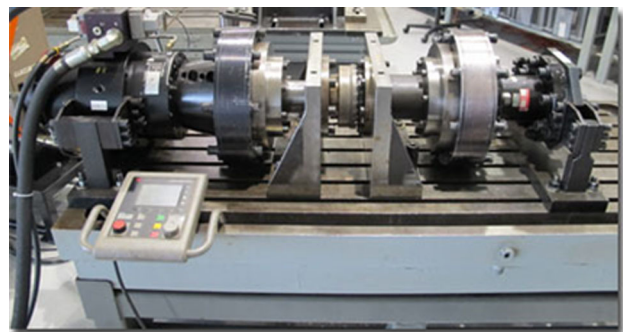
Fig. 1 Torsional fatigue system

Table 1 Fatigue test conditions of specimens 1 to 5

Specimen	Fatigue procedure (Nm)	Cycles	Failure mode
01	+40 to +1116	100,180	Helical fracture through oil hole
02	+40 to +1116	96,536	Helical fracture through oil hole
03	+40 to +1116	79,963	Helical fracture through oil hole
04	+40 to +1116	95,828	Helical fracture through oil hole
05	+40 to +1116	83,876	Helical fracture through oil hole

Fig. 2 Macroscopic upper view of the fracture surface of the failed shaft which shows torsional fatigue fracture with fracture face 45° to the shaft

with blue arrows). This means that the initiating point is located in the transition zone of the case.

The SEM analysis of the fracture surface confirms that the crack initiates from the oil hole and develops toward the center of the shaft. Figure 5a shows SEM micrograph of the crack initiation point in the oil hole. In the present case, during fatigue testing, once the crack is initiated in the oil hole, it propagates under torsional load over a large portion of the shaft periphery in either direction along the circumference of the shaft. Tracking back the beach marks on the fracture surface, the fracture (failure) origin was determined as transition zone of the case on the cross oil hole.

Figure 5b shows higher-magnification image of the fracture surface near initiation point. In this image, red arrows direct void coalescence which is indications of ductile fracture. Blue and yellow arrows show intergranular and transgranular cracking which are signs of brittle-type fracture and failure. Brittle fracture occurs when the maximum stress in the material reaches a critical value. Intergranular brittle fracture (Fig. 5c) may also occur if the prior austenite grain boundaries are embrittled. That is,
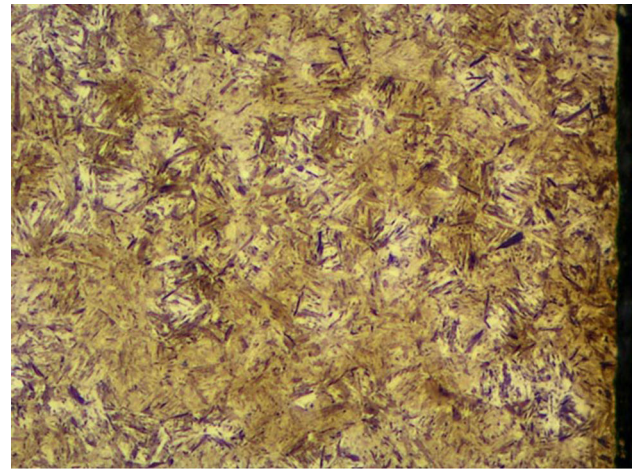
(a)
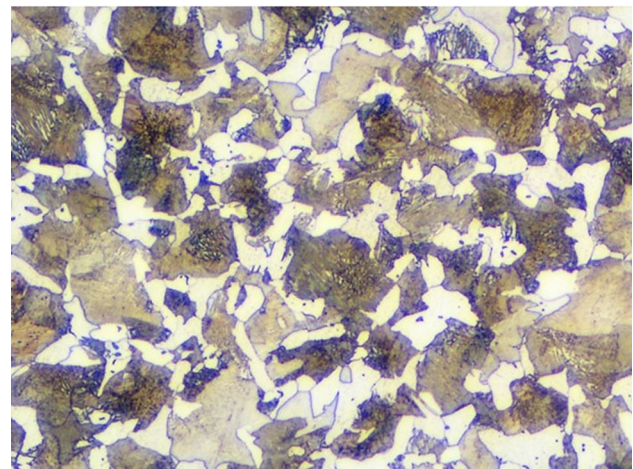
(b)

Fig. 3 Microstructure of the shaft at (**a**) case and (**b**) core

brittle fracture occurs due to the segregation of brittle elements (i.e., hydrogen, phosphor, sulfur) at the austenite grain boundaries during the carburizing process which encourages decohesion of grain boundaries. If hardening occurs through gas carburizing (when a high hydrogen partial pressure is present in the treatment atmosphere), hydrogen absorption may occur resulting in grain boundary embrittlement [9]. The tendency to induce intergranular

1122

J Fail. Anal. and Preven. (2017) 17:1119–1125
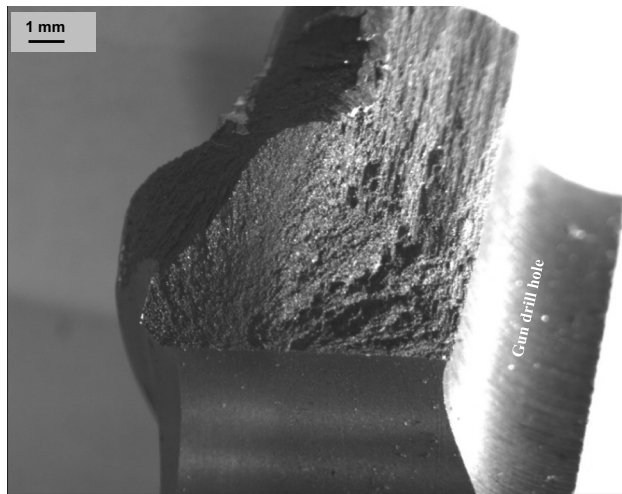
(a)
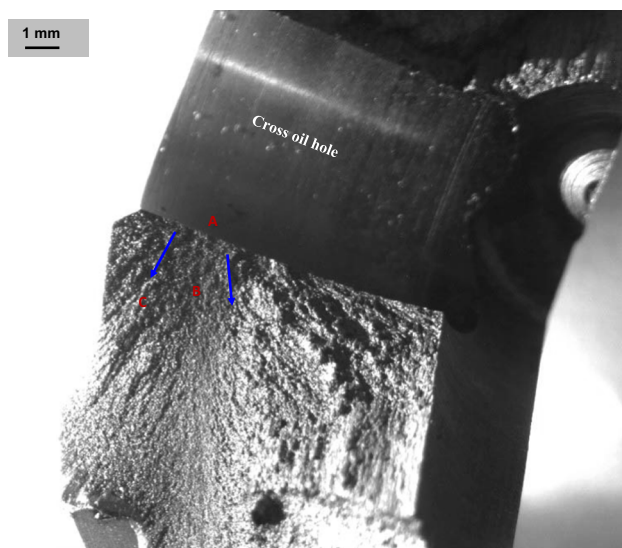
(b)

Fig. 4 Stereomicroscope images of the fracture surface showing crack initiation point and crack propagation path (**a**) upper half, (**b**) lower half

fracture increases with material hardness [10]. The mixed mode of fracture suggests high load and even impact loading as well as low strength (quality) material.

Case Hardness Profile

Case-depth testing often involves implementing a series of hardness tests from the surface of the specimen toward the center. The hardness progression is then plotted on a graph against the distance from the surface. Case hardness depth is an important feature in determining the static and fatigue properties of shafts. Unlike a through-hardened shaft, the main advantage of case hardness is superior wear and
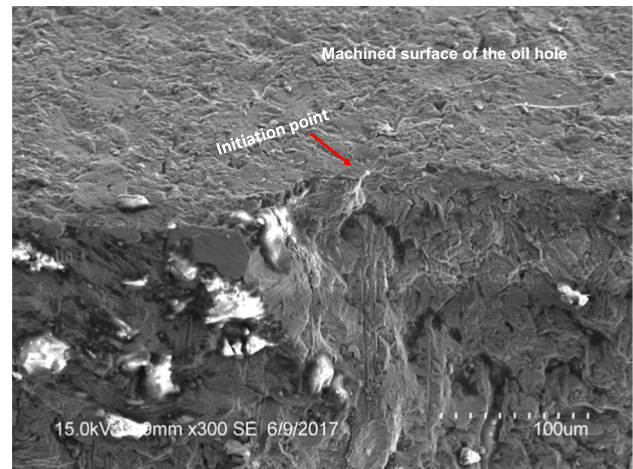
(a)
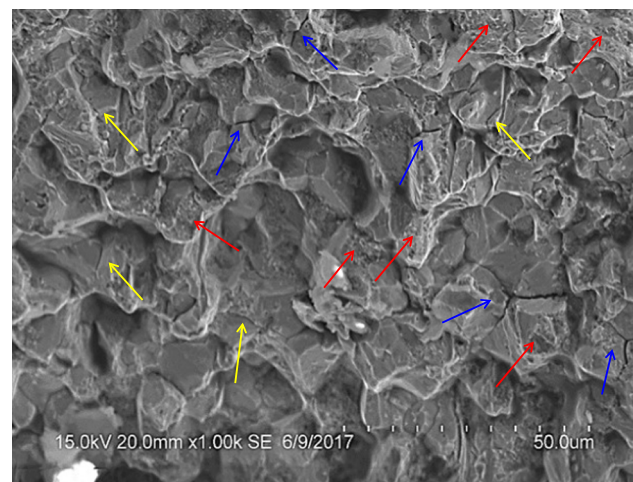
(b)
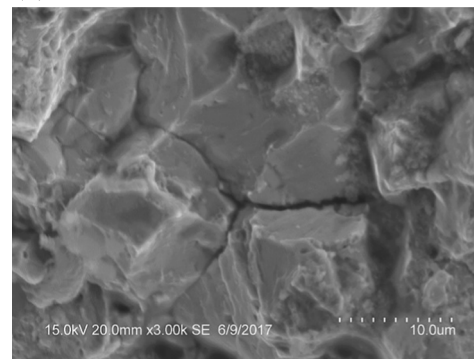
(c)

Fig. 5 (**a**) SEM image of the crack initiation point (shown with letter "A" in Fig. 4), (**b**) spot B in Fig. 4 which shows mixed fracture morphology, (**c**) decohesion of grain boundaries

strength characteristics at the surface of the shaft, while a ductile property at the core.

Case depth is typically measured as *total* and *effective*. The term total case depth refers to the depth of hardness

where the hardened layer reaches the same hardness and properties as the base or core material [11, 12]. Total case depth is typically measured by sectioning the work piece, polishing, and etching to reveal the depth of the hardened layer. The measurements can then be taken visually and measured using a calibrated eyepiece or scale to quantify the total depth.

The term effective case depth refers to the depth where a hardness measurement drops below a specified point. Based on standard ISO 18203: 2016 [13], the case hardness depth describes the vertical distance from the surface to a layer with a limit hardness of 550 HV. The hardness will then continue to decline until the "total" case depth is reached. The hardness at the effective depth is specified based on the characteristics required and the hardenability of the material. Effective case depth specified to ensure the sufficient layer of hardened layer supports surface. This cannot be achieved using just total case depth.

Both effective and total case must be considered to optimize shaft performance. Effective case appears to be the best predictor of torsional strength, while total case is the best predictor of fatigue life [14, 15]. The relationship between case depth and torsional strength is certain, but there is a considerable amount of scatter or variation. Torsional strength does increase with case depth, but only to a point; then, hardening deeper does not necessarily enhance the torsional strength.

Figure 6 shows the case hardness profile of the shaft. The case depth, measured at 550 HV, and the total case are recorded to be 3.1 and 4.5 mm, respectively. Mechanism of crack formation, theoretical approach, is shown in Fig. 7 which, schematically, displays two different induction case depths, (1) solid line and (2) dashed line. The applied stress is shown as a straight line from zero at the center to a maximum at torsional stress at the surface. As seen in the above photograph, at certain depth, case torsional strength is lower than torsional stress (between A–C on diameter for case depth 1); this is where shaft fails. If case depth is pushed deeper (case depth 2), failure area A–C will move closer to the shaft center, to B–C. Torsional stress at depth at which failure occurs (Δ_1) is accordingly pushed down to Δ_2. This means that the failure area is located now in lower stress zone which will increase fatigue life. It is worth mentioning that excessive hardening, deeper than case 2 in this situation, will not necessarily be beneficial because the part will, most probably, fail from the surface due to the significant brittleness. That is, the hypothetical case depth 2 is the optimum case depth. In addition, by hardening too deep, the residual surface compressive stress may be reduced. Another way of reducing area of the material strength below the applied stress is to raise core hardness, which maintains stress curve higher and, thus, reduces the
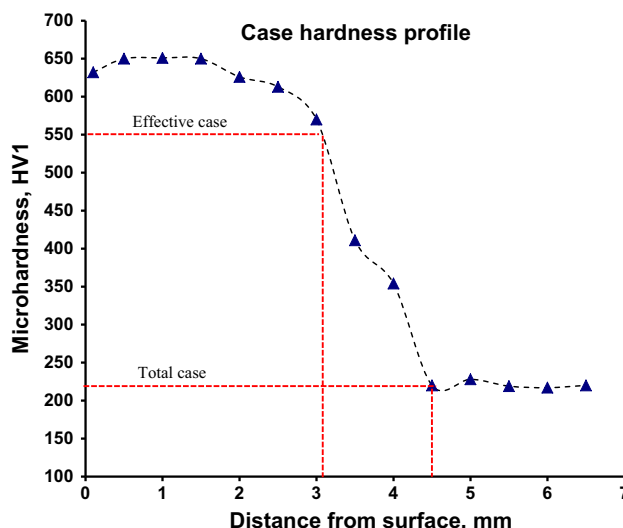

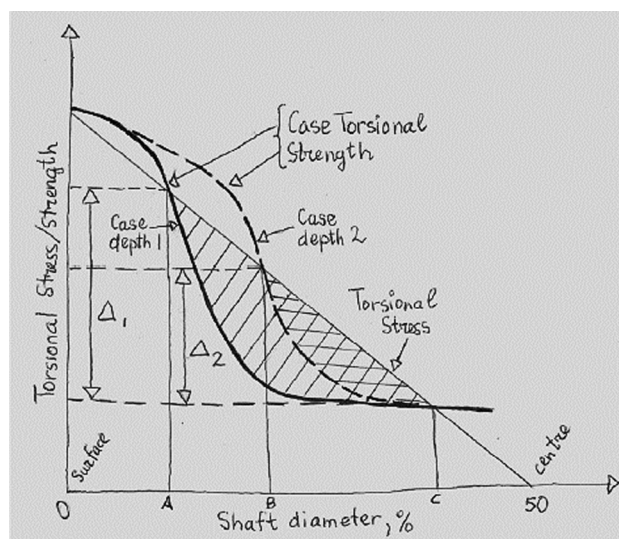Fig. 6 Case hardness profile; the case depth is measured at 550 HV$_1$ to be 3.1 mm

Fig. 7 Mechanism of crack formation (theoretical approach) for this specific case

difference between torsional stress and strength lines which also extends the fatigue life.

Finite Element Analysis (FEA)

For the purpose of FEA, the material properties were considered as $E = 206.8$ GPa and $v = 0.29$. Also, there is only one load case considered in the FEA as torque input is equal to 515 Nm (Fig. 8). No bending loads were taken into consideration as their magnitude was

1124

J Fail. Anal. and Preven. (2017) 17:1119–1125

unknown to us. Model was fixed in radial direction, in axial direction at the end surface of the carrier flange and in rotational (see Fig. 8 which shows the load and boundary conditions of the model). In critical areas, mesh size is 0.3–0.5 mm. Global mesh size was 2 mm. Tetrahedral second-order 3D elements were used in the

analysis. The FEA confirms that the high stress locations of the shaft are mostly around the small lubrication holes. Figure 9 shows the overall stress contour of the shaft. The minimum and maximum stresses were measured as 16.9 and 972.1 MPa at the oil hole, respectively (Fig. 10).
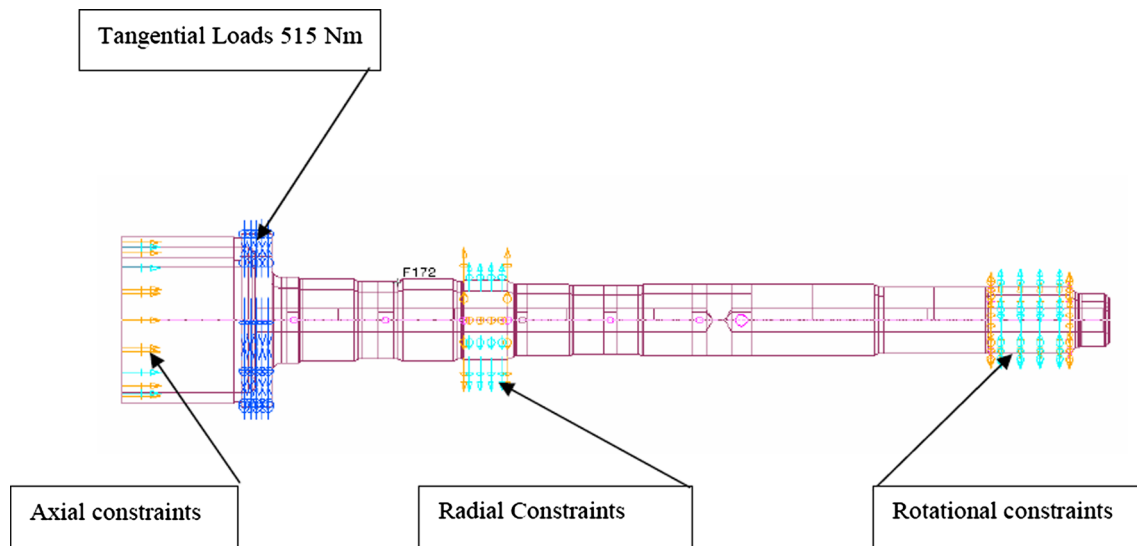
Fig. 8 Loads and boundary condition

Fig. 9 Overall stress contour of the shaft

Von Mises

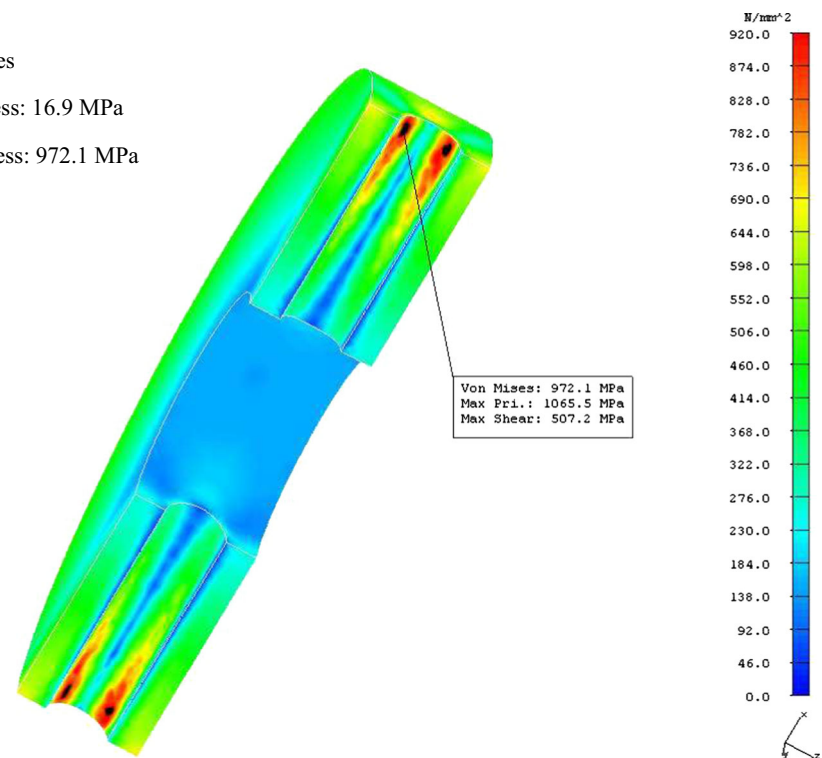Min. Stress: 0.0 MPa
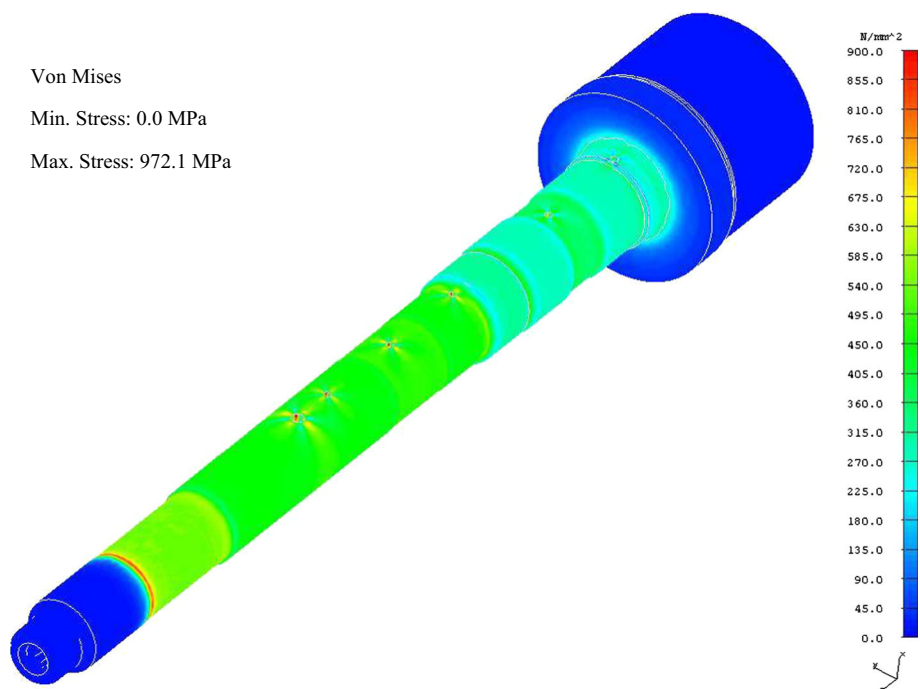
Max. Stress: 972.1 MPa

Fig. 10 Stress contour of the oil hole

Von Mises

Min. Stress: 16.9 MPa

Max. Stress: 972.1 MPa

Remedial Actions

Based on the above-mentioned analyses, the following remedial actions are proposed to improve the fatigue life of the shaft during actual service conditions.

- Analysis of failure showed that transition zone of the case on the cross oil hole is where fatigue failure starts.
- Premature fatigue failure happened because torsional strength in this area is lower than torsional fatigue stress.
- To extend fatigue life, reduction of torsional fatigue stress in the transition zone of the case is required.
- One of the solutions is to make case depth deeper, thus pushing transition zone of case into area of lower torsional stress (i.e., closer to the shaft center).
- Quench delay was extended in this case. As a result, case depth went deeper which resulted on average 40–50% fatigue life increase.
- If fatigue life has to be further improved, in addition to above approach, it is suggested to target higher core hardness as 95 Rb is somewhat soft to withstand any load. By increasing core hardness to above 20 Rc torsional strength of the case would be moved toward higher values (dashed area on figure above with respect to torsional stress will be reduced), thus improving fatigue life too.

References

1. X. Xiaolei, Y. Zhiwei, D. Hongxin, Eng. Fail. Anal. **13**, 1351–1357 (2006)
2. J. JianPing, M. Guang, Eng. Fail. Anal. **15**, 420–429 (2008)
3. M. Godec, D.J. Mandrino, M. Jenko, Eng. Fail. Anal. **16**, 1252–1261 (2009)
4. C. Moolwan, S. Netpu, Proc. Social Behav. Sci. **88**, 154–163 (2013)
5. G. Atxaga, A.M. Irisarri, Eng. Fail. Anal. **17**, 714–721 (2010)
6. H.-S. Han, Eng. Fail. Anal. **44**, 285–298 (2014)
7. S.K. Bhaumik, R. Rangaraju, M.A. Parameswara, M.A. Venkataswamy, T.A. Bhaskaran, R.V. Krishnan, Eng. Fail. Anal. **9**, 457–467 (2002)
8. S. Li, J. Yang, A. Chang, C. Zhang, Y. Gao, M. Wu, X. Wu, M. Li, J. Zhang, Mater. Sci. Forum **850**, 101–106 (2016)
9. H. Streng, C. Razim, J. Grosh, Influence of hydrogen and tempering on the toughness of case-hardened structures, in G. Krauss, editor, *Carburizing: processing and performance* (Colorado, Lakewood, 1989), p. 311–3117
10. G. Straffelini, L. Versari, Eng. Fail. Anal. **16**, 1448–1453 (2009)
11. Standard J423_1998 (02) *Methods of Measuring Case Depth*
12. ASM Handbook, Volume 4A, Steel Heat Treating Fundamentals and Processes J. Dossett and G.E. Totten, editors, Introduction to Surface Hardening of Steels
13. ISO 18203:2016, Steel-determination of the thickness of surface-hardened layers
14. G.A. Fett, Metal Prog. **127**, 49–52 (1985)
15. G.A. Fett, Heat Treat. Prog. **9**, 15–19 (2009)